

**Survey of Degradation Modes of Candidate Materials
for High-Level Radioactive-Waste Disposal Containers**

**Volume 8
Weldability of Copper-Based Alloys**

**D. B. Bullen and G. E. Gdowski
Science & Engineering Associates, Inc.
Pleasanton, Calif.**

**H. Weiss
Lawrence Livermore National Laboratory
Livermore, Calif.**

June 1988

DISCLAIMER

This report was prepared as an account of work sponsored by an agency of the United States Government. Neither the United States Government nor any agency thereof, nor any of their employees, makes any warranty, express or implied, or assumes any legal liability or responsibility for the accuracy, completeness, or usefulness of any information, apparatus, product, or process disclosed, or represents that its use would not infringe privately owned rights. Reference herein to any specific commercial product, process, or service by trade name, trademark, manufacturer, or otherwise does not necessarily constitute or imply its endorsement, recommendation, or favoring by the United States Government or any agency thereof. The views and opinions of authors expressed herein do not necessarily state or reflect those of the United States Government or any agency thereof.

LAWRENCE LIVERMORE NATIONAL LABORATORY
University of California • Livermore, California • 94550

MASTER

Contents

List of Volumes of the Survey	iv
Acronyms	v
Executive Summary	vii
Abstract	1
1. Introduction	1
2. Welding Metallurgy	2
2.1 Basic Metallurgy of the Copper-Based Candidate Alloys	2
2.2 Welding of Copper-Based Alloys	4
2.2.1 CDA 102	5
2.2.2 CDA 613	7
2.2.3 CDA 715	14
3. Alternative Methods of Welding	21
4. Ranking of the Candidate Materials	23
5. Acknowledgments	23
6. References	24

List of Volumes of the Survey

This is Volume 8 of the report *Survey of Degradation Modes of Candidate Materials for High-Level Radioactive-Waste Disposal Containers*. The titles of all of the volumes are as follows:

Overview

Volume 1: Phase Stability

Volume 2: Oxidation and Corrosion

Volume 3: Localized Corrosion and Stress Corrosion Cracking of Austenitic Alloys

Volume 4: Stress Corrosion Cracking of Copper-Based Alloys

Volume 5: Localized Corrosion of Copper-Based Alloys

Volume 6: Effects of Hydrogen in Austenitic and Copper-Based Alloys

Volume 7: Weldability of Austenitic Alloys

Volume 8: Weldability of Copper-Based Alloys

Acronyms

AWS	American Welding Society
BWR	boiling-water reactor
CDA	Copper Development Association
CHLW	commercial high-level waste
DHLW	defense high-level waste
GMAW	gas metal arc welding
GTAW	gas tungsten arc welding
HAZ	heat-affected zone
MIG	metal inert gas
NNWSI	Nevada Nuclear Waste Storage Investigations Project
NWMP	Nuclear Waste Management Program
ppm	parts per million
PWR	pressurized-water reactor
TIG	tungsten inert gas
UTS	ultimate tensile strength

Executive Summary

The candidate materials for the fabrication of containers for the disposal of high-level radioactive waste include three copper-based alloys: CDA 102 (oxygen-free copper), CDA 613 (Cu-7Al), and CDA 715 (Cu-30Ni). This volume reviews the technical literature on the welding of these alloys for the Nuclear Waste Management Program. A number of potential problems associated with welding are identified. These problems do not appear to preclude the application of the copper-based alloys in the fabrication of containers for high-level radioactive-waste storage. The effects of welding on the austenitic candidate materials are reviewed in Volume 7.

The high-purity copper alloy, CDA 102, is difficult to weld since very high heat input is required to compensate for the high thermal conductivity of this material. The significant preheat requirements of conventional welding techniques lead to excessive oxidation of the material. CDA 102 is also prone to embrittlement because of oxide formation when welded in an atmospheric environment. The use of an inert shield gas is required to prevent oxide formation and the associated reduction of cuprous oxide by hydrogen, which results in the formation of water vapor and porosity. The use of a filler material with a deoxidizer or a high-purity copper with a residual deoxidizer, such as CDA 122, might be necessary if high-purity copper is selected as the metal barrier material.

The aluminum bronze candidate material, CDA 613, appears to have significant ductility problems in the temperature range of 400 to 600°C. Brittle failure over this temperature range is thought to be a result of the segregation and precipitation of impurity elements during the welding process. This segregation and embrittlement phenomenon is exacerbated by the repeated thermal cycling produced in multipass welds. The welding of aluminum bronze alloys also requires the use of inert gas shielding to prevent the formation of an aluminum oxide scale, which is insoluble in most flux materials. These oxide particles can become entrapped in the melt and result in weld embrittlement. Aluminum bronze welds have also been shown to dealloy in an acidic corrosion environment over time, which could lead to significant corrosion problems if these conditions occurred in a repository.

The cupronickel candidate alloy, CDA 715, is also prone to problems associated with dealloying. Fusion-line cracking was noted in cupronickel welds as a result of segregation of major alloying elements and impurities. Partial melting, associated with localized solute segregation, was noted as a probable cause of hot cracking in this material. Some research indicates that trace elements, such as lead, sulfur, bismuth, selenium, phosphorus, and tellurium, can be tolerated with the use of nickel filler wire under proper welding conditions. However, the tolerance threshold to trace impurities when nickel filler materials are used is highly dependent upon the thermal gradient. Cupronickels were also identified as being prone to atmospheric contamination, which causes porosity in weldments if proper inert gas shielding is not employed. Because of a relatively wide solid-solution freezing range, cupronickels are also prone to coring, which results in subsolidus tearing that can lead to cracking.

Alternative welding methods that limit heat input and yield relatively small heat-affected zones (HAZs) are also reviewed. Electron-beam welding is identified as a possible method of limiting solute segregation and partial melting due to impurity eutectic formation through the low total heat input required for this process. Electron-beam welding is completed in a vacuum environment, thus eliminating the need for a shielding gas to prevent the formation of porosity from entrapment of hydrogen or water vapor. In addition, electron-beam welding is an autogenous process, requiring no filler material. Inertial or friction welding is also identified as a potential joining alternative. This process requires no special surface preparation and is relatively insensitive to part configuration and welding parameters. There is no fusion on the macroscopic scale and therefore no traditional fusion zone. This feature precludes solute segregation since there is no melt zone. Further development work is required if friction welding is to be applied to the closure of high-level radioactive-waste containers.

On the basis of the available information, the relative weldability of the copper-based alloys is: CDA 715 (best) > CDA 102 > CDA 613 (worst).

Survey of Degradation Modes of Candidate Materials for High-Level Radioactive-Waste Disposal Containers

Volume 8: Weldability of Copper-Based Alloys

Abstract

Three copper-based alloys, CDA 102 (oxygen-free copper), CDA 613 (Cu-7Al), and CDA 715 (Cu-30Ni), are being considered along with three austenitic candidates as possible materials for fabrication of containers for disposal of high-level radioactive waste. The waste will include spent fuel assemblies from reactors as well as high-level reprocessing wastes in borosilicate glass and will be sent to the prospective repository at Yucca Mountain, Nevada, for disposal. The containers must maintain mechanical integrity for 50 yr after emplacement to allow for retrieval of waste during the preclosure phase of repository operation. Containment is required to be substantially complete for up to 300 to 1000 yr. During the early period, the containers will be exposed to high temperatures and high gamma radiation fields from the decay of high-level waste. The final closure joint will be critical to the integrity of the containers.

This volume surveys the available data on the metallurgy of the copper-based candidate alloys and the welding techniques employed to join these materials. The focus of this volume is on the methods applicable to remote-handling procedures in a hot-cell environment with limited possibility of postweld heat treatment. The three copper-based candidates are ranked on the basis of the various closure techniques.

On the basis of considerations regarding welding, the following ranking is proposed for the copper-based alloys: CDA 715 (best) > CDA 102 > CDA 613 (worst).

1. Introduction

The Nuclear Waste Management Program (NWMP) at Lawrence Livermore National Laboratory is responsible for the development of the engineered barrier design to meet the Nuclear Regulatory Commission licensing requirements for the containment of high-level nuclear waste. This waste will include (1) spent fuel from civilian nuclear power plants, namely, fuel assemblies from pressurized-water reactors (PWRs) and boiling-water reactors (BWRs), (2) commercial high-level waste (CHLW) in the form of borosilicate glass containing commercial spent-fuel reprocessing wastes, and (3) defense high-level waste (DHLW), also contained in borosilicate glass. The engineered containment package is being designed for emplacement at a repository in the Topopah Spring Member of the Paintbrush Tuff at the Yucca Mountain site in Nevada. The design of the containment package is based on

criteria provided by the Nevada Nuclear Waste Storage Investigations (NNWSI) Project. The reference horizon is located 350 m below the ground surface and 200 m above the static water table. The composition of the vadose water makes the repository conditions slightly oxidizing.

The Metal Barrier Selection and Testing Task of the NNWSI Project is responsible for selecting the materials to be employed in the waste-package container and possibly the borehole liner. Six candidate materials are currently under consideration: three austenitic alloys and three copper-based alloys. The austenitic materials are Type 304L stainless steel, Type 316L stainless steel, and Alloy 825. The copper-based alloys are CDA 102 (oxygen-free copper), CDA 613 (Cu-7Al), and CDA 715 (Cu-30Ni). The selection of the final metal barrier material is dependent

upon the stability of these materials in the repository environment.

The design criteria for the metal barrier require that the waste containers maintain mechanical integrity for a period of 50 yr after emplacement to permit retrieval of the nuclear waste during the preclosure phase of repository operation. The containers are required to provide substantially complete containment for up to 300 to 1000 yr for most containers. This requirement implies limited failure of a few containers. During this containment period, the metal barrier will be exposed to a changing environment. A few years after emplacement, the surfaces of some of the containers will reach a maximum temperature of about 250°C. This temperature will decay to about 150°C within about 100 yr after emplacement. This time period will also include the highest gamma radiation field from the decay of the high-level waste.

The final closure joint will be critical to the integrity of the containers. This joint will be remotely sealed in a hot-cell environment following the insertion of the waste form. The temperature of the spent-fuel waste form must be maintained below about 650°C because of the potential materials interactions that can occur within the fuel assembly. This limitation precludes most forms

of postclosure treatments, such as postweld heat treatment. Therefore, the integrity and long-term stability of the closure seal and the associated heat-affected zone (HAZ) surrounding this seal will have a significant impact on the degradation of the container.

Reviews of the degradation modes of the candidate materials have been completed for the NWMP. These literature surveys address phase stability [1], oxidation and corrosion [2], effects of hydrogen [3], stress corrosion cracking [4, 5], and localized corrosion [4, 6] of the candidate materials under repository-relevant conditions. This volume addresses the effects of joining on the degradation of the copper-based candidate materials. A discussion on the methodology and extent of the literature search can be found in the Overview.*

This volume includes a review of the metallurgy of the copper-based candidate alloys, a review of welding techniques employed to join CDA 102, CDA 613, and CDA 715, and a ranking of the candidates with respect to welding. The final ranking of the various candidate closure techniques for the copper-based alloys is made with respect to repository-relevant conditions and requirements.

2. Welding Metallurgy

The metallurgy of the copper-based alloys is somewhat simpler than that of the iron- to nickel-based austenitic alloys. The compositions of the copper-based candidate materials CDA 102 (oxygen-free copper), CDA 613 (Cu 7-Al), and CDA 715 (Cu-30Ni) are shown in Table 1 [7]. These materials are essentially solid-solution alloys with minor alloying components that can have limited solubilities. The welding process employed to join these materials can have a significant impact on the solubilities of these minor alloying elements and any impurity contaminants. The microstructure introduced as a result of the precipitation of these minor alloying constituents or impurities during welding can produce changes in mechanical properties that can cause failure of the weld due to hot cracking, weld-porosity formation, or embrittlement of the weld and/or HAZ. A review of the metallurgy of the copper-based alloys is provided as a basis for understanding the

micro-structural and metallurgical changes incurred during the welding process.

2.1 Basic Metallurgy of the Copper-Based Candidate Alloys

As noted in Table 1, CDA 102 is essentially a pure material, and it will exhibit few, if any, changes in microstructural or mechanical properties under repository conditions. The mechanical strength of CDA 102 is primarily dependent on the thermomechanical history of the specific part. The higher the degree of cold work, the greater the yield stress and creep resistance. The impurity element that has the greatest effect on

* J. C. Farmer, R. D. McCright, J. N. Kass, *Survey of Degradation Modes of Candidate Materials for High-Level Radioactive-Waste Disposal Containers, Overview*, Lawrence Livermore National Laboratory, Livermore, California, UCID-21362 Overview (1988).

Table 1. Compositions of the copper-based candidate alloys for welding applications [7]. Note: composition shown is percent maximum (unless shown as a range, as a minimum, or as nominal).

Element	CDA 102	CDA 613	CDA 715
Cu	99.95 (min)	92.7 (nom.)	69.5 (nom.)
Fe	—	2.0–3.0	0.4–1.0
Pb	—	0.01	0.02
Sn	—	0.2–0.5	—
Al	—	6.0–7.5	—
Mn	—	0.2	1.0
Ni	—	0.15	29.0–33.0
Zn	—	0.05	0.5
P	—	0.015	0.02
S	—	—	0.02
C	—	—	0.05
Cr	—	0.05	—
Cd	—	0.05	—
Zr	—	0.05	—

CDA 102 is oxygen in the form of Cu_2O precipitates. These precipitates are not wetted by molten copper and hence are found predominantly on the grain boundaries of the as-cast material. The nonwettability of Cu_2O precipitates will also have a significant effect on the welding microstructure produced when attempting to join CDA 102 parts. The introduction of very small amounts of oxygen into the weld melt pool can result in the formation of Cu_2O precipitates that will be swept to grain boundaries during solidification. This phenomenon can result in hot cracking or embrittlement of the weld, which can produce failure of the joint. These oxide precipitates are examined in greater detail in Sec. 2.2.1, which deals with welding CDA 102.

Figure 1 shows the copper-aluminum equilibrium phase diagram [8]. This binary system exhibits several interesting phase transformations between about 10 and 30 wt% aluminum. Note that a eutectoid decomposition occurs at 565°C and approximately 12 wt% aluminum. This is a martensitic transformation at slow cooling rates, where the β phase transforms to α_1 and γ_2 phases. This transformation might prove important when considering the conditions that will occur in the HAZ of a closure seal. Figure 2 [9] shows a partial phase diagram for the copper-aluminum system in the region around 9 to 16 wt% aluminum in copper. This figure extends the lower tempera-

ture of the phase diagram to 0°C (273 K) and highlights the complex phase transformations that take place in these materials. The effects of phase stability and transformation on the mechanical properties of the copper-aluminum system are dealt with in detail elsewhere [1].

The copper-nickel equilibrium phase diagram exhibits solid-solution behavior throughout the entire composition range, as shown in Fig. 3 [1, 10, 11]. This means that no precipitate phases are present under equilibrium conditions, which suggests that this material might have advantages when considering the HAZ at the closure seal of the container. The only possible disadvantage in the copper-nickel system during the welding process is that of dealloying during solidification. As noted in Fig. 3, the solidification composition for Cu-30 at.% Ni is approximately 50 at.% Ni. This suggests that the composition of the alloy that initially solidifies might be higher in nickel content than the final portion of the melt that solidifies. This variation in alloy composition might result in localized solute segregation and the eventual dealloying of the material in the welded region. Dealloying could lead to significant corrosion and/or stress corrosion cracking, depending on the residual stresses introduced during the closure process. These possibilities are discussed further in Sec. 2.2.3, which addresses the welding of CDA 715.

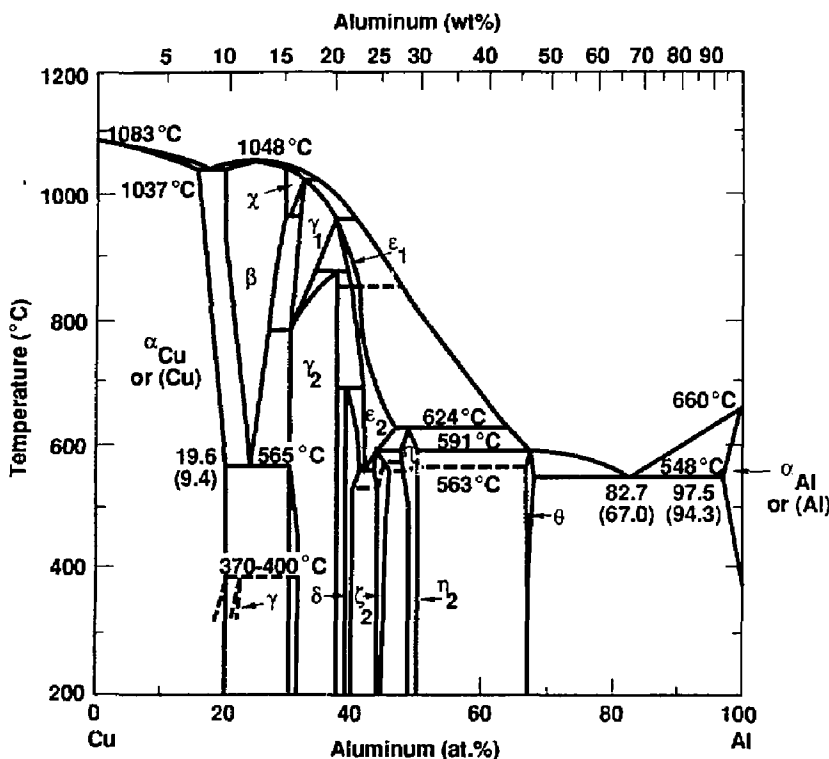


Figure 1. Copper-aluminum equilibrium phase diagram [8].

The mechanical properties of the copper-based candidate alloys are important factors in determining the final design geometry and material requirements of the container. A comparison of the tensile strength as a function of temperature is given for annealed specimens of the copper-based candidate materials in Fig. 4 [12]. Note that at high temperatures, CDA 715 has significantly higher tensile strength than does CDA 613 or CDA 102. Above approximately 175°C, the tensile strength of CDA 715 surpasses that of CDA 613. Under repository conditions (25°C < T < 250°C), CDA 613 and CDA 715 have significantly higher tensile strength than CDA 102. These mechanical properties provide a baseline for a comparison of the effects of welding on the mechanical and microstructural behavior of these materials in a repository environment. It is assumed that the closure seal or weld will have mechanical properties similar to those of the base metal.

2.2 Welding of Copper-Based Alloys

Numerous review articles in the technical literature [13-17] and metallurgical texts [18, 19] have addressed the joining of copper and copper-based alloys. Lancaster [18] reviewed the history of welding commercially pure copper and noted that gas welding was the first fusion process to be applied successfully. Joints of acceptable strength were initially made possible through the use of phosphorus-deoxidized copper, such as CDA 122. More recently, inert-gas welding, employing argon, helium, or nitrogen as a shielding gas, has greatly increased the applicability of fusion welding to copper alloys. Coated electrode welding of aluminum bronze has been successfully demonstrated. However, Lancaster [18] also states that coated electrode welding has not been generally successful in producing satisfactory results in pure copper or cupronickels. These conclusions may not be entirely correct with respect to

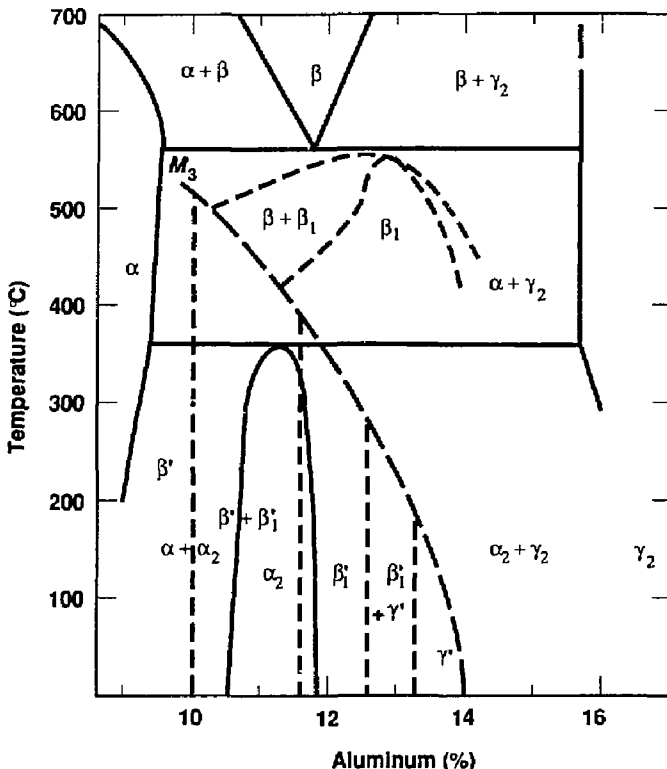


Figure 2. Partial copper-aluminum equilibrium phase diagram [9].

cupronickel alloys. Witherell [20] notes that "response of covered electrode welding of cupronickel alloys is excellent and is routinely done to the most stringent fabrication codes, including nuclear (ASME Section III and U.S. Navy BuShips)."

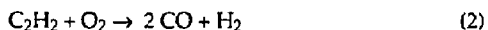
2.2.1 CDA 102

Porosity in the melt zone of pure copper is a major cause of metal embrittlement and weld failure. This porosity is usually due to the reduction of copper oxide by hydrogen. At elevated temperatures (above about 500°C), copper oxide is reduced by hydrogen to form steam in the reaction:



This reaction has been noted to occur in both liquid and solid metal. It is particularly evident in

oxyacetylene welding, where hydrogen, formed in the first stage of combustion, is available from the reaction:



This mechanism of embrittlement of copper, which was noted as *Wasserstoffkrankheit* or "hydrogen sickness" in early research on copper metallurgy completed by the Germans [21-26], is extensively discussed in another volume of this report [3]. Beginning with the early investigations of Mattsson and Schuckher [21], the effects of hydrogen on the mechanical properties and microstructure of pure copper have been extensively documented.

The degradation of high-purity copper exposed to a hydrogen environment is due to the formation of cavities on the grain boundaries. The mechanism, initially proposed by Ransley [23], was experimentally verified by

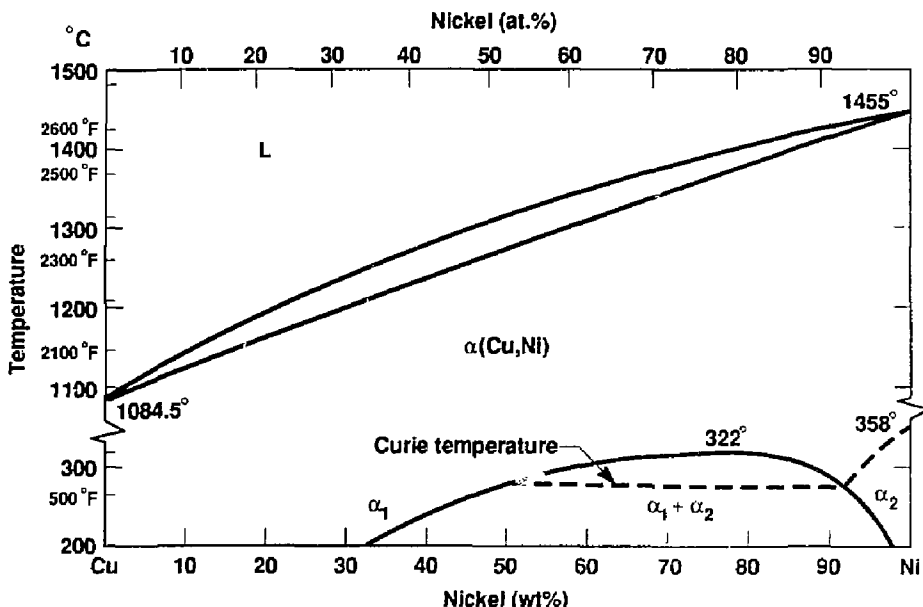


Figure 3. Copper-nickel equilibrium phase diagram [1, 10, 11].

Mattsson and Schuckher [21]. This mechanism describes the formation of cuprous oxide (Cu_2O) in the molten copper as the metal solidifies. Since Cu_2O is not wetted by molten copper, the oxide is swept to the grain boundaries during the solidification process. The Cu_2O is not an extremely stable compound, with a Gibbs free energy of formation (ΔG_f) of ~ 34.9 kcal/mole. When the cast material is exposed to a hydrogen environment, the Cu_2O is reduced, forming water vapor ($\Delta G_f = -57.796$ kcal/mole) and metallic copper. Since the density of metallic copper is significantly greater than that of Cu_2O , a void space is readily formed at the site where the Cu_2O reduction occurred. This void is stabilized by the water vapor molecule and begins to grow as more Cu_2O reduction occurs along the same grain boundary.

This process leads to the beaded microstructure observed at the grain boundaries in nearly all cases in which hydrogen sickness has been documented. The formation of cavities on the grain boundaries quickly leads to a significant reduction in the ductility of the copper, and ultimately to brittle intergranular fracture. The effects of hydrogen sickness have been noted in pure copper with an oxygen content as low as 22 ppm [25].

There are a number of methods that prevent the degradation of copper by hydrogen sickness. The addition of small amounts of alloying elements such as zirconium, boron, phosphorus, or magnesium can tie up the oxygen in the form of stable oxides. These oxides cannot be reduced by hydrogen, thus preventing the formation of water vapor molecules within the copper matrix. Another advantage of these oxides is that they are wetted by molten copper. This wetting prevents the segregation of oxides to the grain boundaries during solidification following the welding process.

The reduction of weld porosity by the addition of a deoxidant suggests that oxygen (and the steam reaction) might be an important factor in the failure of welds. However, an analysis of the gases trapped in the pores of welded copper indicates that the primary entrapped species is hydrogen [18]. It must also be noted that steam formation requires the simultaneous presence of hydrogen and oxygen in the weld pool. The sources of these two elements in the inert-gas-shielded welding of copper have not been established. Therefore, the exact mechanisms leading to porosity in welded copper are the subject of debate.

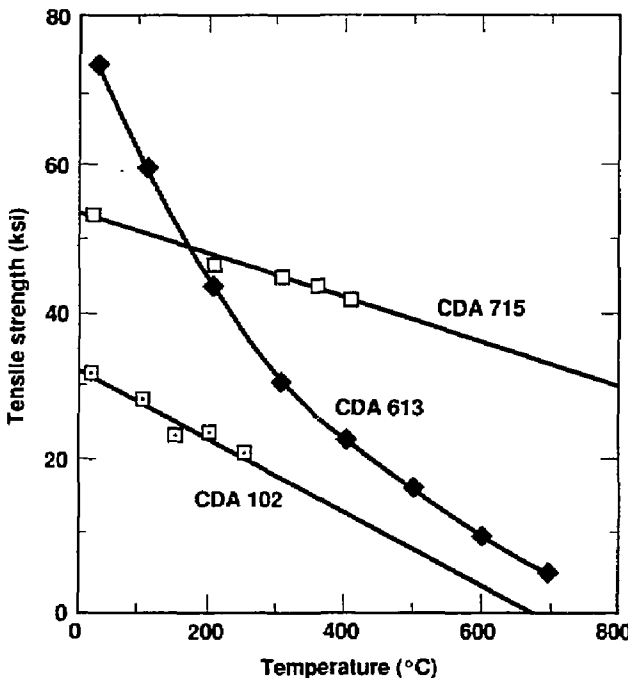


Figure 4. Tensile strength as a function of temperature for the copper-based candidate materials [12].

Dawson [17] reviews the methods that have been successfully employed to weld many commercial copper alloys. This study notes that when attempting to weld oxygen-free copper, such as CDA 102, an extremely high energy density is required because of the excellent thermal conductivity of the metal. This high energy density can lead to oxidation over a wide area, which might penetrate and embrittle the grain boundaries. The primary objective in welding this grade of copper should be to reduce the heat input to an absolute minimum consistent with satisfactory fusion. Methods such as friction welding (with the limited heating of the part) or electron-beam welding (which is completed in a vacuum) are most likely to produce satisfactory joints with limited oxidation. These methods are discussed in Sec. 3.

2.2.2 CDA 613

The attractive corrosion-resistant and scaling-resistant properties of aluminum bronzes are conferred by the presence of a tenacious surface oxide film consisting essentially of aluminum oxide. This oxide is an extremely refractory material

that is insoluble in most welding fluxes. Prior to the advent of the inert-gas-shielded process, this insolubility led to great difficulty in attempts to weld these materials. In the inert-gas-shielded process, the oxide film is dispersed by the action of the arc. The entrapped oxide particles, which were a common problem in gas-welded copper, have been essentially eliminated by careful application of the inert-gas metal-arc process.

A significant amount of information addressing the welding of aluminum bronzes has been identified in the literature [13, 14, 16, 17, 27-32]. Early work by Moore and Taylor [13] and Terry and Taylor [14] addressed the application of the inert-gas-shielded metal-arc process to welding aluminum bronze and cupronickel. These studies addressed the welding parameters required for sound welds.

Terry and Taylor [14] reviewed the metallurgy of the welding process for the aluminum bronze and cupronickel alloys. Their study addressed the effects of various welding parameters and filler materials on the integrity of welds in copper alloys. Hot cracking, which is caused by

brittleness in high-temperature phases of the alloy, and root embrittlement, which is the embrittlement of the root weld pass by subsequent weld passes due to thermal cycling, were noted in some of the aluminum bronze alloys welded. However, it was noted that variation in the filler materials and thermal history of the sample had a significant impact on the success of the weld. The aluminum bronze welds produced in this study were more likely to undergo hot cracking or root embrittlement with an increase in the number of weld passes. Embrittlement was noted at the weld root near the initial weld pass when welding 1-cm-thick (0.375 in.) aluminum bronze with a seven-pass weld. Similar embrittlement was not observed for a five-pass weld in the same material. This observation was attributed to the stabilization of brittle intermetallic phases by minor impurities introduced during the welding process. This study concluded that the susceptibility of aluminum bronzes to hot cracking is small, and correct application of the inert-gas metal-arc process should cause little trouble in practice.

Subsequent studies by Lancaster and Slater [28] and Clews [29-31] addressed the issue of cracking of aluminum bronze welds in great detail. An initial study by Lancaster and Slater [28] identified cracking in aluminum bronze plates welded by argon-arc and inert-gas arc processes. Cracking was observed when the aluminum content of the weld deposit was below a critical level, which was identified as between 6 and 7.5% aluminum. Metallographic evidence suggested that the cracks occurred above the solidus temperature and were caused by the presence of low-melting-point, intergranular films consisting primarily of a β constituent. Embrittlement of multipass deposits made using the inert-gas metal-arc process with Cu-7Al filler wire was also observed. This embrittlement was attributed to the formation of a brittle γ_2 phase as a result of the reheating of successive welding passes.

Further work by Clews [29-31] addressed the metallurgical aspects of welding aluminum bronzes. A majority of this work centered on the weldability of Alloy D, which has a nominal composition of 7% aluminum and 3% iron, with the balance copper. The equilibrium phase diagram for this system is shown in Fig. 5 for a 3% iron content [30]. Note that the composition range for Alloy D is very similar to that of CDA 613. Clews completed an extensive review of the mechanical properties of aluminum bronze welds and parent metal at room temperature and

elevated temperature and of the corrosion behavior of aluminum bronze welds [29]. This study employed the British alloy, Alloy D, which has essentially the same composition as CDA 613. These alloys were welded using the argon-arc and carbon-arc processes. These welding processes resulted in a slight depletion in the aluminum content of the welds. Specimens of Alloy D welded with Alloy D filler wire were exposed to solutions of 5% H_2SO_4 for a period of 434 days. These samples exhibited localized dealuminification and, in one case, severe corrosion of the weld.

Clews [29-31] also completed an extensive experimental program addressing the mechanical properties of aluminum bronze alloys at elevated temperatures to better understand the effect of multiple temperature cycles on the failure of weld metals. Figure 6 shows the ductile-brittle transition for Alloy D weld metal [29]. Note the almost complete loss of ductility at a temperature of about 400°C. There is a recovery in ductility at temperatures above 700°C, but ductility as high as that at room temperature is not regained. This behavior is consistent with the observation of brittle failure modes in multipass welds of aluminum bronze alloys with a composition of about 7% aluminum.

The effect of simulated weld thermal cycles on the mechanical properties of Alloy D at room temperature and elevated temperature was also documented in this study, as shown in Fig. 7 [29]. This figure shows the reduction in ultimate tensile strength (UTS) and elongation, and the reduction in area for Alloy D specimens subjected to thermal cycles equivalent to from 1 to 9 weld passes. It can be seen from the figure that specimens subjected to 1 or 2 temperature cycles tend to be stronger and less ductile than those cycled for 3, 4, 6, 7, or 9 cycles, with the comparison being made at room temperature. Clews noted the anomalously high strength behavior for the 5-cycle specimen, and noted that further work was required to determine whether this effect is real. Microstructural evaluation of the welded Alloy D material indicated no noticeable difference in the amount of β phase in each weld pass. In summarizing this work, Clews suggests that the brittle behavior of Alloy D over the temperature range of 400 to 600°C, which this study called hot shortness, is associated with the presence of one or more equilibrium-segregated impurities that melt or become brittle in this temperature range. These impurity phases then become soluble in the matrix as the temperature rises during welding

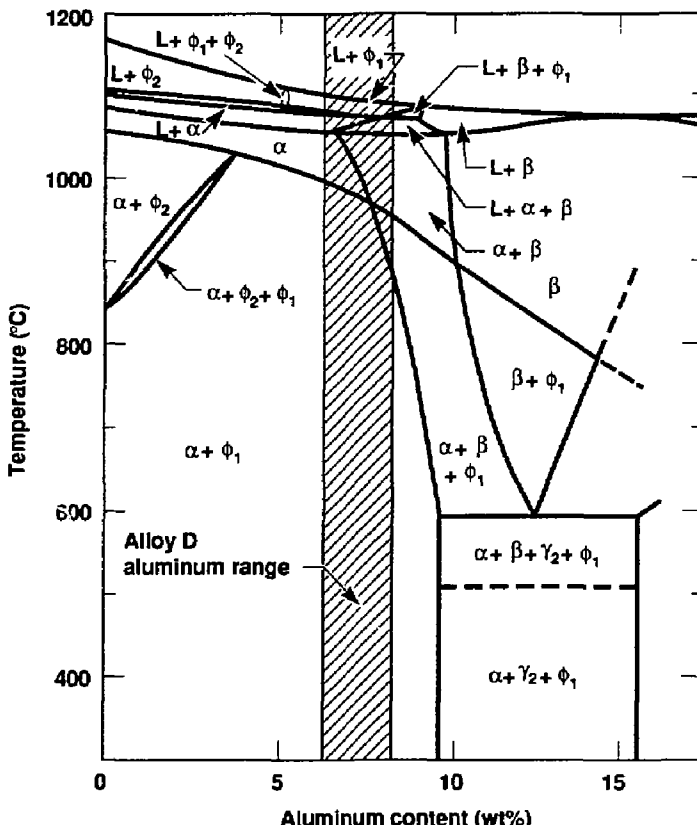


Figure 5. Copper-aluminum-iron equilibrium phase diagram (section at 3% iron) [30].

and separate out at the grain boundaries as the temperature falls. This phenomenon produces the observed embrittlement over this temperature range.

Clews [31] completed further studies of the effects of aluminum and impurities on the hot tensile strength of Alloy D. Clews completed mechanical testing of various compositions of Alloy D with differing contents of aluminum and various impurities. Materials were prepared with concentrations of aluminum ranging from 6 to 8% and small amounts of lead and bismuth to simulate inferior grades of copper. Samples were also prepared with small amounts of uranium added to the lead- and bismuth-contaminated alloys. Tensile tests were completed on these materials and on samples prepared from inert-gas-shielded metal-arc weld deposits of the alloy contaminated with lead and bismuth and the alloy containing

lead, bismuth, and uranium. Figure 8 [31] shows the variation in mechanical properties as a function of temperature for pure Alloy D. Note that for high temperatures, the ductility of Alloy D increases with increasing aluminum content. Figure 9 [31] shows the effect of aluminum content on the mechanical properties of the impure Alloy D samples (lead and bismuth added) at elevated temperatures. Note the overall decrease in ductility with the addition of the lead and bismuth impurities. Also note that the high-temperature ductility still increases with increasing aluminum content. Clews concluded by stating:

1. Hot ductility of wrought aluminum bronze increased as the aluminum content increased from 6 to 8%.
2. Small amounts of lead and bismuth were harmful at all temperatures.

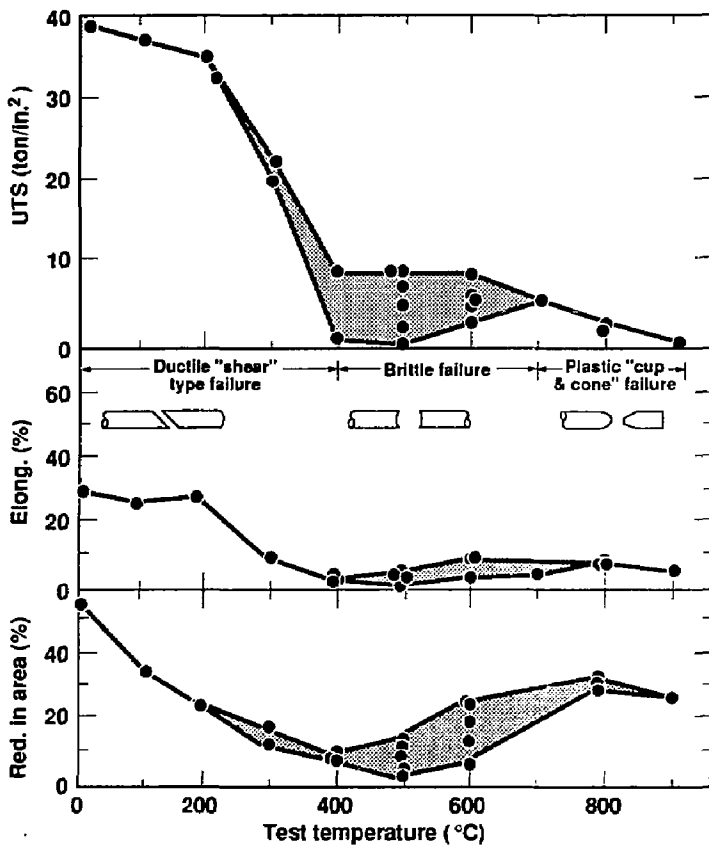


Figure 6. Ductile-brittle transition in Alloy D weld metal [29].

3. Uranium additions overcome the harmful effects of lead and bismuth in wrought aluminum bronze, and the addition of uranium to the pure alloy is beneficial.
4. The beneficial effect of uranium in Alloy D was lost when the alloy was deposited as a weld metal. However, an increase in the uranium content of the filler wire might result in better weld metal properties.
5. When Alloy D containing 2.5% iron is relatively free of lead and bismuth, it has adequate ductility for welding irrespective of its aluminum content. Small amounts of lead (0.005%) and bismuth (0.001%) make it unsuitable for welding.

Clews [31] also completed a study of the effect of composition and strain rate on the cracking

of welded Alloy D in order to model cracking during welding and solidification. This study investigated the effects of variation in composition, thermomechanical history, and strain rate on the performance of Alloy D plates during welding. Clews showed that, with differing composition and thermomechanical treatment, similar samples of Alloy D exhibit widely different weldability.

The impact of thermomechanical history can be better understood by considering Fig. 5. Material with a high aluminum content, when rolled at a high temperature followed by rapid cooling, can give rise to an $\alpha\beta$ microstructure. Metallographic investigation noted that the β phase can be distributed in stringer form during rolling. This heterogeneous microstructure, which can be very directional in nature, can significantly alter the strength and ductility of

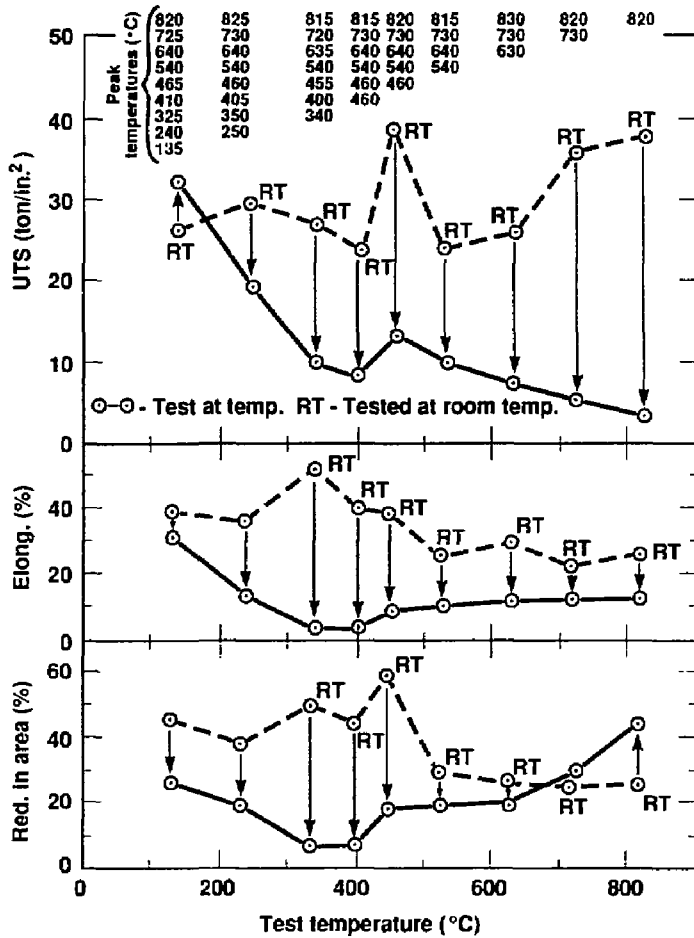


Figure 7. Effect of simulated weld thermal cycles on the room-temperature and elevated-temperature properties of Alloy D [29].

Alloy D at temperatures of approximately 450°C. Unweldable Alloy D plates have been found to have an elongation value of less than 10% at 450°C because of the effects of the heterogeneous or homogeneous nature of the microstructure resulting from the thermomechanical history of each plate. The only method identified in this study [31] that can successfully predict the weldability of different Alloy D plates is a high-temperature mechanical stress test at relatively high strain rates. Plates with less than 10% elongation in a tensile test at 450°C were identified as unsuitable for welding.

Difficulties in welding aluminum bronzes, similar to those identified by Clews for Alloy D, have been summarized in a brief review by Wold [16]. This review noted that welding of CDA 613 requires moderate preheating to avoid setting up severe stress differentials caused by the material's relatively low ductility and low heat-transfer rates. The review by Dawson [17] suggested several welding procedures for aluminum bronze alloys. Dawson states:

1. No preheat and low inter-run temperatures are recommended to reduce the problems

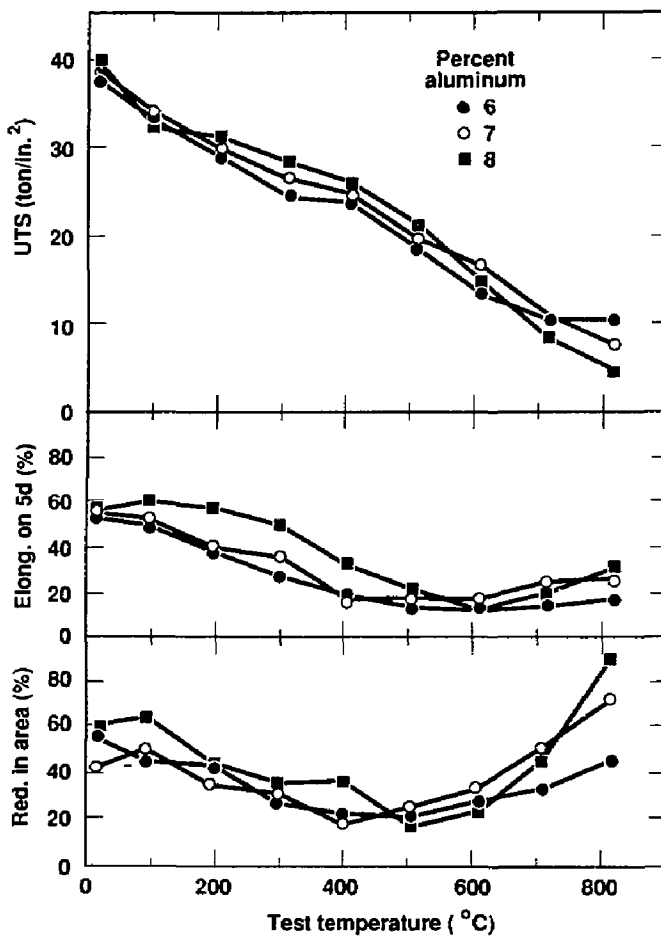


Figure 8. Effect of aluminum content on the elevated-temperature mechanical properties of pure Alloy D [31].

of hot cracking, particularly of single-phase alloys.

2. Helium shielded-gas tungsten-arc welding with direct-current electrode negative working is recommended for all grades in preference to alternating-current with argon, particularly for thin-to-thick sections and cast material. The helium arc is hotter, and facilitates more rapid deposition and faster welding, and consequently, less heat spread.
3. Filler metal selection must be given particular care because single-phase alloys are

prone to weld cracking in multipass welds and because the achievement of matching corrosion resistance across the weld zone is normally critical. When possible, the more hot ductile two-phase filler metal should be deposited for the main weld runs and capped finally by the single phase alloy to match bulk structure.

4. Postweld heat treatment is recommended to fully restore the corrosion resistance of the complete structure in critical applications. This normally consists of a higher-temperature soak to homogenize

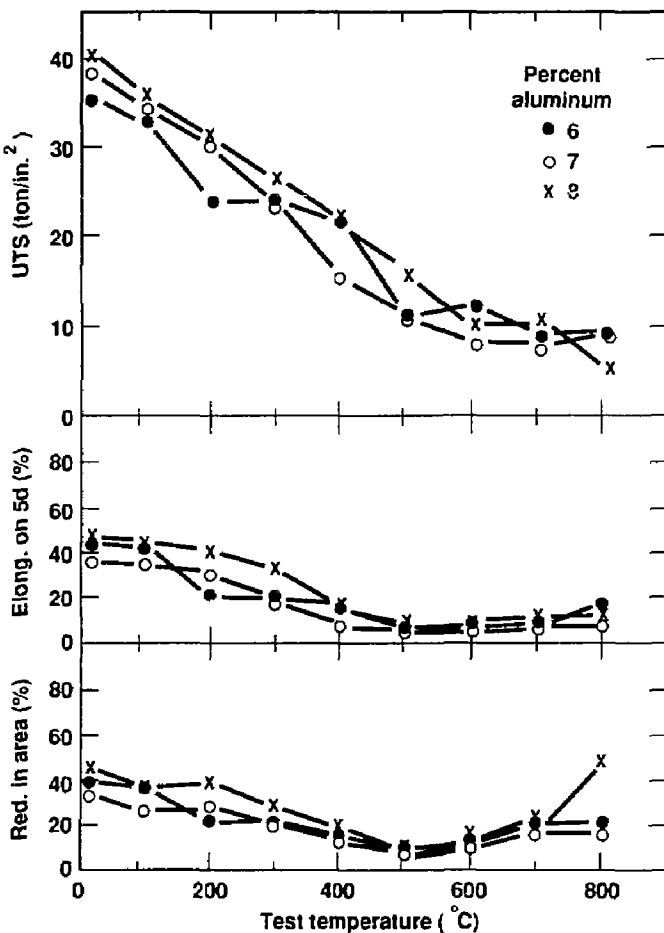


Figure 9. Effect of aluminum content on the elevated-temperature mechanical properties of impure Alloy D [31]. The alloys were contaminated with small amounts of lead (0.005%) and bismuth (<0.001%).

the structure, and a lower-temperature treatment below the transformation temperature of the alloy to develop the full mechanical and corrosion-resistant properties.

Current industrial practices employed in welding aluminum bronze alloys have specifically addressed the issue of alumina oxide inclusions within the fusion zone. Medley [33] notes that the protective aluminum oxide coating on aluminum bronze alloys can be successfully disrupted by employing a helium or helium/

argon mixture in a 90/10 or 80/20 ratio as the shield gas in the tungsten inert-gas (TIG) welding process. Utilization of the metal inert-gas (MIG) welding process, where the filler wire creates the arc, results in an "atomization," yielding a spray mode that disrupts the oxide coating. Medley [33] notes that if a forehand method of application is used, a dense clean weld, free from oxides, results from the MIG welding process.

It should be noted that there exists a wide variation of welding parameters and practices that have been applied to the joining of CDA 613

and all of the aluminum bronzes. This variation in methods is due to the lack of hot ductility of some of the high-aluminum alloys and the variation in the corrosion resistance required of the part to be welded.

2.2.3 CDA 715

Numerous studies have addressed the welding properties and practices for cupronickel alloys [13–15, 18, 34–42]. Lancaster [18] notes that the most suitable welding process for the cupronickels is inert-gas-shielded tungsten-arc welding. With this method, cracking is not a serious problem, and porosity is minimized by using a filler rod containing a deoxidant (where a suitable deoxidant is titanium). Weaver and Imperati [15] noted that both inert-gas-shielded tungsten-arc welding and inert-gas-shielded metal-arc welding are readily applicable to cupronickels. This review also noted that oxyacetylene welding of cupronickels, though seldom employed, is also possible with proper materials preparation and technique. The review also noted that the inert-gas-shielded metal-arc process of welding the cupronickels has been described extensively in the literature. Inert-gas-shielded metal-arc welding has been designated gas metal arc welding (GMAW) by the American Welding Society (AWS). Inert-gas-shielded tungsten-arc welding has been designated gas tungsten arc welding (GTAW) by the AWS.

Early studies [13, 14] of the welding of copper alloys reviewed the weldability of cupronickel alloys by a variety of welding processes. Moore and Taylor [13] studied the application of the inert-gas-shielded metal-arc welding process to a number of copper alloys, noting the effects of various filler-wire compositions and welding parameters. Welding of the cupronickels with this method required the use of filler wires containing strong deoxidants to prevent weld porosity. This was one of the initial studies that proposed the full commercial application of this welding technique for copper alloys.

A further study by Terry and Taylor [14] investigated the metallurgical factors affecting the weldability of cupronickel alloys. The binary cupronickel alloy consists of an entirely single-phase solid solution, as shown in Fig. 3. Small alloy additions of iron and manganese are included to increase corrosion resistance. Welding of this solid-solution material with normal cooling rates usually leads to a weld-metal structure that is cored. Cupronickel alloys are also susceptible to

hot cracking at elevated temperatures, particularly if the components to be welded are subject to a high degree of restraint. The risk of cracking is considerably increased by the presence of certain impurities, the most significant being sulfur, lead, and phosphorus. Although phosphorus enhances the weldability of pure copper by acting as a deoxidant, significant concentrations of copper impurities can produce an embrittled microstructure and result in cracking. This study compared CTAW, GMAW, and gas welding processes for cupronickel alloys and concluded that, with the application of suitable filler materials (containing small amounts of strong deoxidants such as titanium or aluminum), inert-gas-shielded arc processes produce sound, strong joints.

Hawthorne and Burth [34] also recognized the importance of the application of the correct filler material to welding cupronickel alloys. This study included extensive mechanical testing of cupronickel alloys welded with the inert-gas-shielded tungsten-arc process and the inert-gas-shielded metal-arc process. The utilization of Cu-30Ni filler wire for both welding processes when welding 70-30 and 90-10 cupronickel alloys resulted in satisfactory joints in all cases. Tensile tests and bend tests of all welded specimens yielded satisfactory strength and ductility.

Witherell [35] completed an extensive investigation of fusion-line cracking in cupronickel alloys. This study addressed the effect of impurity materials on the weldability of Cu-30Ni. Approximately 250 compositions of cupronickel were produced to determine the effect of impurity elements on weld microstructure. Other factors that were identified as controlling the degree of segregation and thus having an impact on fusion line cracking were weld-energy input and filler metal composition. This study concluded:

1. Fusion-line cracking in cupronickel welds is primarily the result of low-melting-point segregates that form at the weld interface when certain trace elements or impurities (such as phosphorus, lead, cadmium, bismuth, selenium, and tellurium in Cu-30Ni) are present in the base metal in sufficient quantities.
2. The cracking seems to occur when the stresses generated by the cooling mass of weld metal exceed the strength of the low-melting-point segregates. Trace elements that have low solid solubility in copper, or form low-melting-point eutectics with copper, are chiefly responsible.

- The use of nickel or a high-nickel copper filler, or welding conditions that promote fast cooling rates and rapid solidification of the deposited weld metal, tend to favor the segregation of low-melting-point constituents and thereby increase the likelihood of fusion-line cracking.

Matthews [37] completed an investigation of the cause of hot cracking in Cu-30Ni tubesheet materials to determine the hot ductility of the weld metal and heat-affected zone (HAZ). In this study, the results of Varestraint and hot-ductility tests were compared with the frequency of hot cracking observed in the HAZ of tube-to-tubesheet welds. The purpose of this study was to identify methods for evaluating the weldability of various copper alloys and to identify

metallurgical factors that influence the hot-crack susceptibility of copper-nickel tubesheet materials.

This study employed the Varestraint test, in which a weld bead is deposited on a plate supported as a cantilever beam, and the composite is simultaneously bent to a radius determined by the curvature of a replaceable die block, as shown in Fig. 10 [38]. This procedure introduces a reproducible, augmented strain of known magnitude. The results of the Varestraint tests were compared with those of hot-ductility tests. Hot-ductility tests are completed by subjecting the specimen to a programmed thermal cycle and then loading the specimen in tension at some pre-selected point in the cycle. A welding cycle was selected for this experiment to represent the

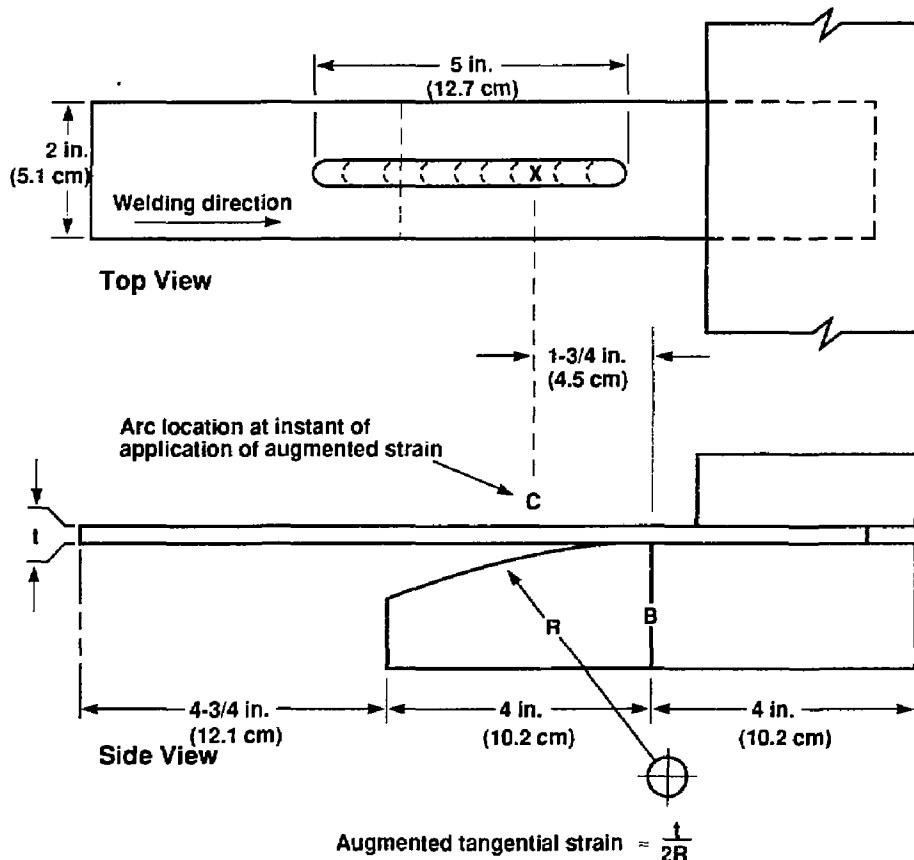


Figure 10. Simplified sketch illustrating the Cu-30Ni Varestraint testing [38].

thermal conditions in the HAZ of the base metal. Metallographic examinations of samples from both methods were completed after each test. This investigation also addressed the effects of impurities in the weld microstructure on the hot cracking of the welds. Small amounts of silver (0.056%) were introduced into the microstructure on forging employed in these tests, the results of which are given below.

The results of this investigation [37] verified the utility of the application of the Varestraint test to determining the weldability of copper-nickel alloys. This study concluded:

1. The Varestraint test successfully differentiated and ranked the hot cracking susceptibility of copper-nickel overlay cladding (and three heats of copper-nickel forgings), the weldability of which was known from prior welding experience.
2. Varestraint test results significantly correlated with the results obtained on the same material heats utilizing the hot ductility test. A large mid-temperature range ductility loss experienced for both on-heating and on-cooling test conditions corresponds to a high level of cracking produced on the Varestraint apparatus.
3. The maximum high-temperature ductility of Cu-30Ni forgings exists between 982 and 1121°C (1800 and 2050°F). At 1177°C (2150°F), the ductility of copper-nickel rapidly drops to zero.
4. The microstructure of the tubesheet material must be considered when attempting to weld crack-free, tube-to-tubesheet joints where high strain is present in the ligament area.
5. High silver content in Cu-30Ni forgings may contribute to poor weldability.

Another early study of the weldability of Cu-30Ni also employed the Varestraint test. Lee et al. [38] studied the feasibility of applying the Varestraint test to evaluate the heat-to-heat variations in the weldability of cast Cu-30Ni alloy. This study compared the Varestraint test to the military specification MIL-C-20159B to determine the effects of welding parameters and trace-element contamination on the hot-cracking sensitivity of Cu-30Ni alloy. These tests were supplemented by metallographic and electron microprobe analyses. Welding was completed by utilizing the inert-gas-shielded tungsten-arc process without the addition of filler metal. The results of these tests yielded cracks in the fusion

zone, the HAZ, and the base metal adjacent to the HAZ. Microprobe analysis indicated the segregation of low-melting-point impurities such as lead, sulfur, and phosphorus, to the grain-boundary and subgrain-boundary regions of the fusion zone and HAZ. This microsegregation of impurities was considered as the principal factor in determining the cracking location.

An extensive study of microsegregation in Cu-30Ni alloys was completed by Savage et al. [39-41]. Savage et al. [39] completed electron microprobe analysis of Cu-30Ni welds to study the distribution of solutes throughout the fusion zone. Principles of solidification mechanics were applied to explain the observed distributions of elemental concentrations. Figure 11 [39] shows a schematic of the solidification process for the conditions at which redistribution of solute in the liquid phase is by diffusion only and there is no diffusion of solute in the solid phase. Note that this produces a solute-concentration transient spike during solidification. Electron microprobe analysis of weld specimens of Cu-30Ni prepared from autogenous gas tungsten-arc welds noted significant segregation of impurity and major alloying elements, as shown in Fig. 12 [39]. The presence of the solute concentration transient spike, predicted by solidification mechanics, can be seen in the concentration profile for zinc and lead.

This study [39] concluded that welds made in Cu-30Ni exhibit extensive solute segregation in the fusion zone and that a steady-state solute concentration gradient exists ahead of the solid-liquid interface during solidification of welds. Attempts were also made to determine the elemental distribution of solutes and major alloying elements in the fusion zone. The range of nickel content noted in the fusion zone was from 25% at the boundary to 38% at the center.

Additional work by Savage et al. [40] hypothesized a mechanism of partial melting that results in microsegregation of major and impurity elements in Cu-30Ni welds. A schematic for the mechanism of partial melting in a single-phase alloy (such as Cu-30Ni) is shown in Fig. 13 [40]. The mechanism for partial melting was described by noting that, in the presence of point-to-point variations in solute content in the base metal, the effective melting temperature would vary, as shown in Fig. 13. Two typical temperature gradients are superimposed on the schematic, showing point-to-point variation in the effective melting temperature. Note that at the localities where the

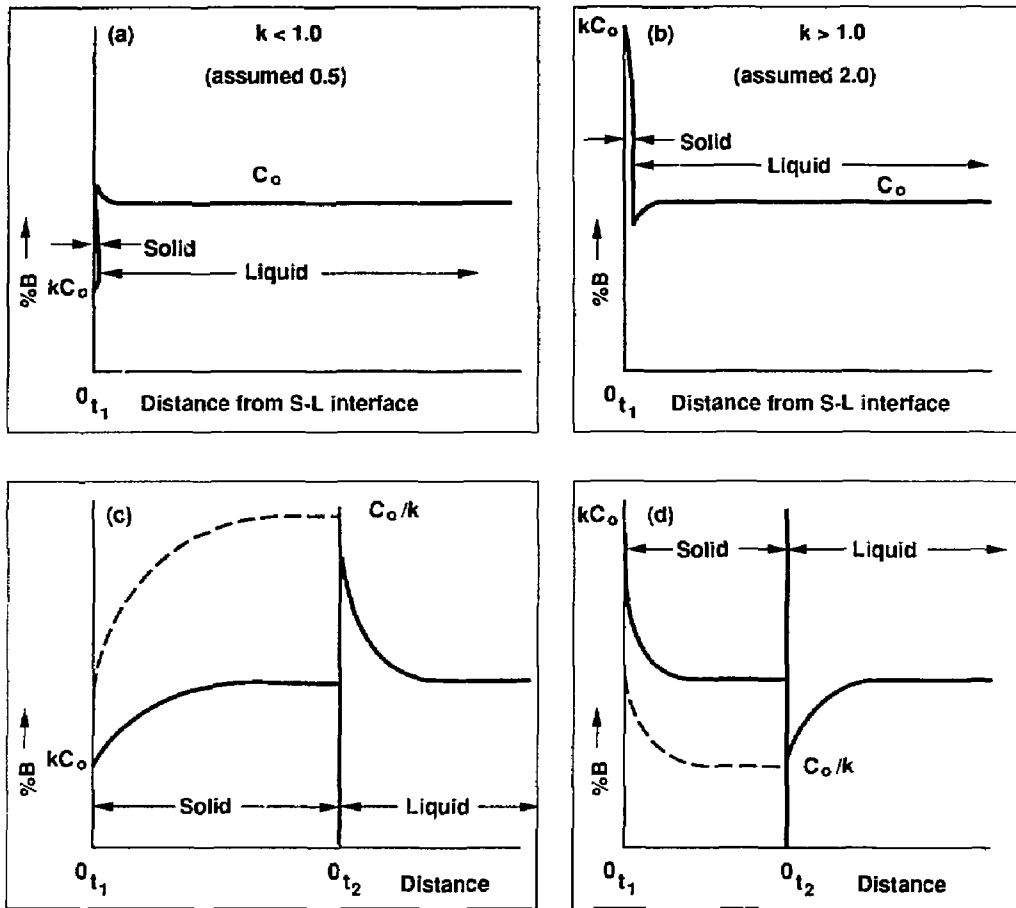


Figure 11. Schematic showing transient phenomena during initial solidification [39].

effective melting temperature is below the instantaneous temperature, localized melting will occur. The extent of melting and the separation between localized molten regions will determine the distance over which grain boundaries can migrate before becoming pinned.

The width of the partially melted region depends on both the temperature gradient produced adjacent to the weld and the magnitude of the peak-to-peak variations in solute concentration in the original base metal. The influence of peak-to-peak variations in solute concentration can be seen in Fig. 14 [40]. For a homogeneous Cu-30Ni alloy, the solidus and liquidus temperatures correspond to 1166 and 1238°C, respectively. Thus,

the partially melted region for the perfectly homogeneous alloy would extend over a 72°C (130°F as shown in Fig. 14) interval of the temperature gradient beyond the locus of the liquidus, i.e., the fusion line. However, if there were a 5% variation in the nickel content due to residual segregation in the base metal, the nickel-rich regions would exhibit a liquidus of 1149°C, and the nickel-depleted regions would exhibit a solidus of 1260°C. Thus, the partially melted region would extend over a 111°C (200°F as shown in Fig. 14) interval of the temperature gradient beyond the locus of the liquidus. Thus, microsegregation can significantly increase the extent of the partial melt zone.

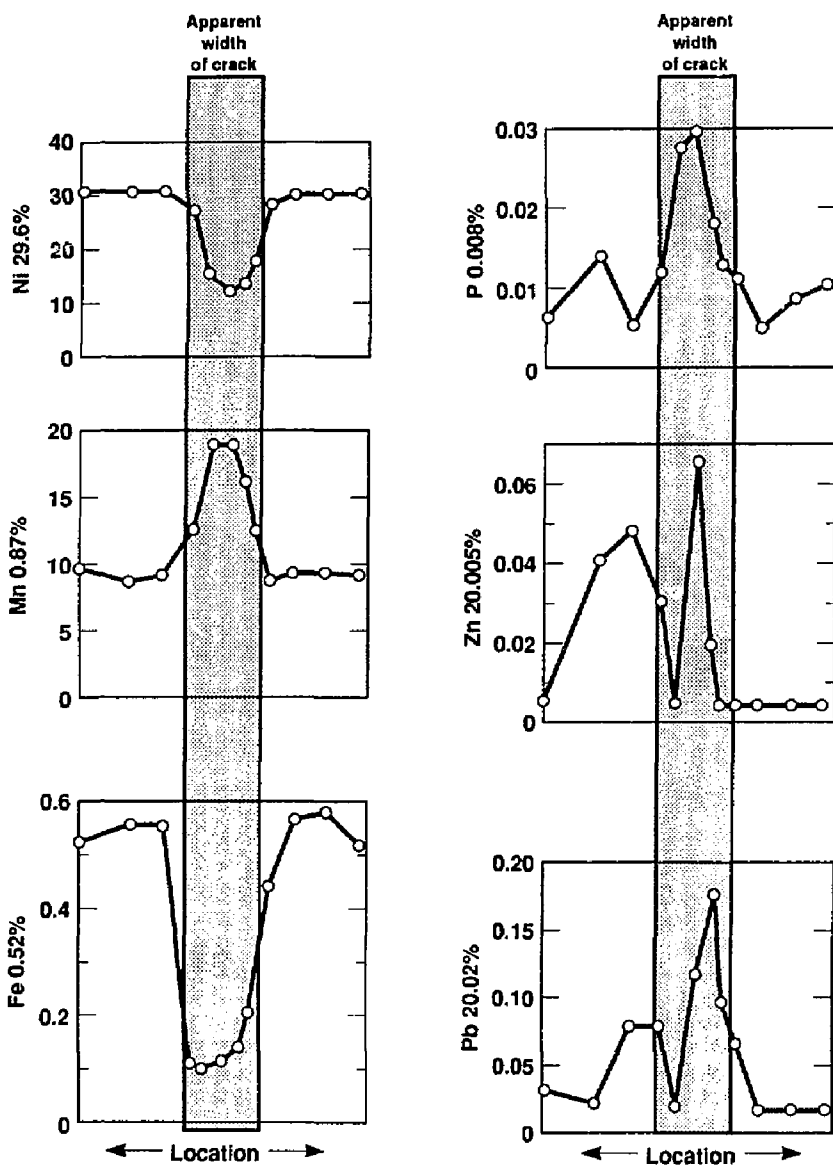


Figure 12. Plots of composition vs location for six elements across crack in Varestraint specimen [39].

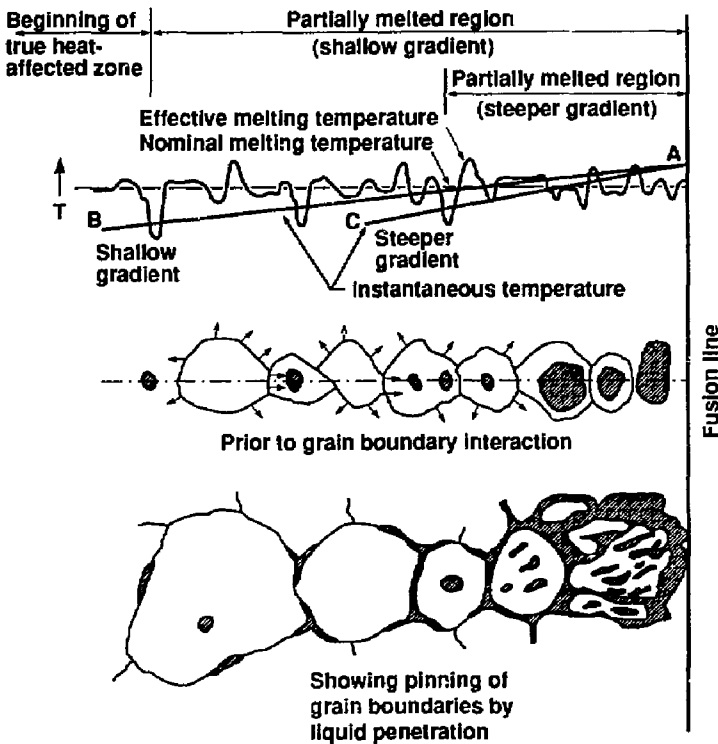


Figure 13. Proposed mechanism for partial melting in a single-phase alloy [40].

This study employed electron microprobe analysis techniques to determine the variation in alloy composition over the melt and partial-melt regions of a Varestraint test weld produced by an autogenous-gas tungsten-arc process on cold-rolled Cu-30Ni alloy. This study concluded:

1. A partially melted region occurs adjacent to the fusion line of welds made in a commercially prepared alloy of Cu-30Ni.
2. Welds made in Cu-30Ni exhibit solute segregation in the partially melted region.
3. Metallographic evidence substantiated the hypothesis of partial melting by observation of grain-boundary broadening and interference with normal grain growth.
4. Electron-beam microprobe analysis of the broadened grain boundary in the partially melted regions shows solute segregation of a form that causes localized reduction of the effective melting temperature.

5. The partially melted region in welds of Cu-30Ni is probably a nucleation site for hot cracking in the base metal adjacent to the weld fusion zone.

Further work by Savage et al. [40] more fully addressed the effects of impurity and alloying elements on the hot-cracking sensitivity of Cu-30Ni alloys. Noting that small additions of iron, manganese, phosphorus, and lead have been employed in solution to strengthen copper-nickel alloys, this investigation completed a parametric study of the effects of various combinations of these alloying elements on the propensity for hot cracking in these alloys when welded. This work also attempted to determine whether hot-cracking resistance could be improved by thermomechanical treatment involving cold work and recrystallization. Small additions of phosphorus (0.01%), lead (0.003%), iron (0.25%), and manganese (0.3%)

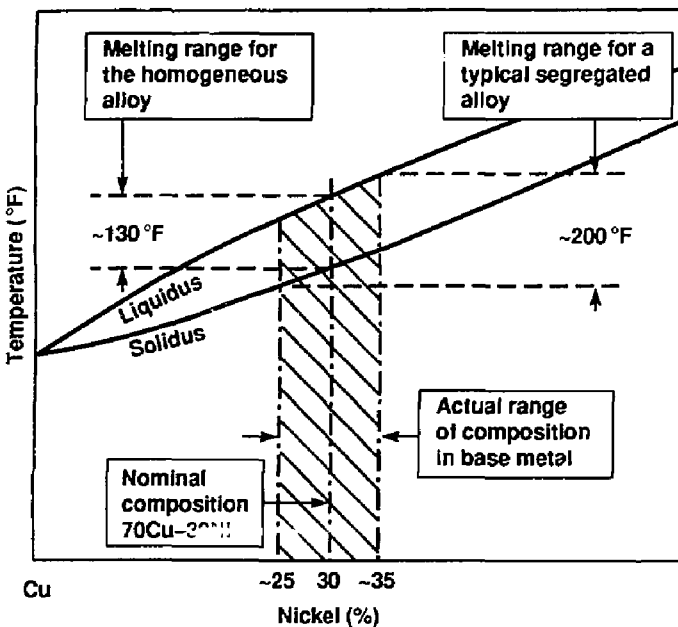


Figure 14. The influence of segregation on the melting range of a binary alloy [40].

were introduced into the Cu-30Ni alloy by employing a gas tungsten-arc remelting process of metal powder compacted in a groove on the surface of a Cu-30Ni plate in an argon dry box. The resulting remelt microstructure was examined using optical metallography, transmission electron microscopy, and electron microprobe analysis to determine the crack density and elemental distributions. Hot cracking was augmented by the addition of phosphorus and manganese. Additions of lead reduced hot cracking, and additions of iron had no effect. Second-order combinations of phosphorus-iron and lead-iron were detrimental, and the combination of phosphorus-lead was the most detrimental of all. The combination of lead-manganese was beneficial in reducing hot cracking.

A recent review [42] of the welding of copper-nickel alloys addressed the accepted industrial practices that might be employed to successfully join these materials. TIG and MIG welding techniques can be successfully employed with proper material purity and weld-surface preparation. This paper reported the maximum impurity concentrations that can be tolerated and still produce sound welds. These impurity

concentrations, shown in Fig. 15 [42], depend on the filler material employed in the weld. When nickel filler material is used, greater levels of sulfur, phosphorus, lead, bismuth, selenium, and tellurium can be tolerated. This study concludes that, with careful welding practices, welding of copper-nickel alloys poses no great problems.

The results of the previous study [42] are not generally accepted in the welding industry. Witherell [43] notes that "tolerance thresholds for trace impurities using nickel filler metals depend upon the thermal gradient (and, therefore, the stress gradient at the heat affected zone) in the welded part. Under conditions where these gradients are steep, tolerance thresholds for nickel filler (viz., of higher solidification temperature) will be lower."

An excellent summary of the problems associated with the welding of copper-nickel alloys was provided in the review article by Dawson [17]. This review suggests that several factors are particularly relevant to the welding of copper-nickel alloys. Dawson states:

1. All grades of these alloys are susceptible to cracking caused by the presence of trace

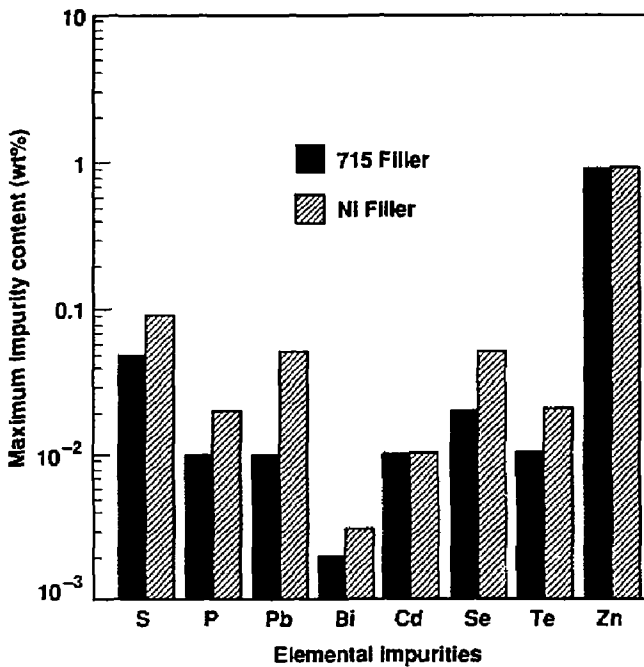


Figure 15. Maximum permissible impurity concentrations when producing sound welds in Cu-30Ni alloy [42].

elements such as lead and sulfur from machine oils, furnace atmospheres, etc., and care must be taken to avoid such contact.

2. Cupronickels are especially prone to atmospheric contamination, causing porosity in weldments. The specially developed filler metals must be used to counteract this effect, and particular attention should be given to effective shielding of both sides of the weld.
3. Helium shielding or argon-helium mixtures are particularly effective in gas tungsten-arc and gas metal-arc welding to enable high weld speeds and reduce the welding time, thus reducing risk of porosity. Direct-current electrode negative work is recommended for gas tungsten-arc welding.
4. Cupronickels are prone to coring as they solidify through a somewhat wide, solid-solution freezing range. This renders them liable to subsolidus tearing, and restraint must be reduced to avoid cracking.

3. Alternative Methods of Welding

As indicated in the papers reviewed in the previous sections, the welding of copper-based alloys is not without drawbacks and some difficulty. The problems of hot cracking, porosity, and microsegregation can all have an impact on

the integrity of the welded joint. Three feasibility studies [44-46] have been completed for Lawrence Livermore National Laboratory which address the fabrication and closure of containers to be employed in the Nuclear Waste

Management Program (NWMP). These studies review alternatives for the fabrication and closure of the high-level nuclear-waste storage containers being designed for use at the Yucca Mountain site in Nevada.

Kundig [44] reviewed the closure requirements of the nuclear-waste container with respect to the copper-based candidate materials and proposed two methods of closure: (1) electron-beam welding, and (2) inertial or friction welding. Both of these methods require relatively low heat input and thus would limit the problems associated with more conventional welding procedures. Low heat input would provide little time for solute segregation and partial melting associated with impurity eutectic formation. Electron-beam welding is an autogenous process, requiring no filler wire. This process is usually completed in a vacuum environment, precluding the requirement for gas shielding and the possibility of porosity from the entrapment of hydrogen or water vapor during the welding process.

Inertial or friction welding was also proposed by Kundig [44] as a means of container closure. Friction welding can be completed without the use of a shielding gas or a vacuum environment. The process is completed by rubbing two metal surfaces together until the frictional heat generated causes them to bond metallurgically. There is no fusion on the macroscopic scale and, therefore, no traditional fusion zone. The bond line has an appearance similar to that of a forged joint. Kundig notes that the advantages of a friction welding process include:

1. The ability to produce high-quality welds consistently.
2. The ready inspectability of the welds.
3. The relative insensitivity of this process to surface contamination.
4. The ability to locate most moving parts outside the hot cell facility.
5. The fundamental simplicity of the process.
6. The ability to measure parameters prior to welding.
7. The relative insensitivity to part configuration and welding parameters.

It should also be noted that there are a number of potential disadvantages associated with the friction welding process. These include:

1. Upset formation (flash) during the welding process: External flash must be removed prior to emplacement of containers.
2. Potential internal crevice formation due to internal flash.
3. Significantly less industrial experience.
4. The container must be designed to resist the thrust and load forces required to complete the friction weld.
5. There may be a significant increase in capital costs to design and build the friction welding system in a hot-cell environment.

Although friction welding is still a developmental process, this study states that there is no indication that it will prove unsatisfactory for nuclear-waste container-closure applications. This study concludes that both friction welding and electron-beam welding appear to be promising alternatives for container closure.

Two other feasibility studies [45, 46] that have addressed the issue of joining the copper-based candidate materials have been completed for the NWMP. These studies include an entire decision-tree analyses for selection of the fabrication and closure processes to be employed by the NWMP. In the report on closure, Stein [45] evaluates five potential closure methods, including friction welding, electron-beam welding, laser-beam welding, gas tungsten-arc welding, and plasma-arc welding. When the decision-tree analysis was applied to the parameters of the requirements of the nuclear-waste repository, friction welding and electron-beam welding were ranked as the top two candidate methods for container closure. These methods were selected primarily for the limited heat-input requirements and the autogenous nature of the welding method.

Alternative closure techniques for copper-based containers have been briefly reviewed in industrial trade journals. Dawson [47] provides an excellent summary of the status of industrial practices employed in the welding of copper and copper alloys. This report includes a brief description of the state-of-the-art of pressure bonding, friction welding, ultrasonic welding, and induction and resistance welding. A more extensive review of applications of friction welding in copper and copper alloys is presented by Nichols [48], who reviews typical welding conditions for the bonding of various copper alloys using friction welding. A review of current

applications of friction-welded copper alloys is also provided.

Wang [49] has completed an extensive review of the friction welding process, addressing the typical welding parameters and materials that can be joined. A review of the specific power and critical initial surface speed for welding certain materials is also provided. This study states that

a specific power of 110 kW/cm^2 (950 hp/in.^2), and a critical initial surface speed of 914 cm/sec (1800 ft/min) are required for the welding of most copper alloys. This study also states that the bond produced in the friction welding process can exhibit strengths as great as that of the base metal.

4. Ranking of the Candidate Materials

Considering the effects of welding alone, the following ranking of the copper-based candidate materials is proposed:

1. CDA 715
2. CDA 102
3. CDA 613

This ranking considers the application of traditional and developmental welding techniques, as documented in this volume.

CDA 715 is judged to be superior since it undergoes less catastrophic degradation and failure with respect to oxide formation and loss of ductility. The microsegregation of alloying elements and impurities and the partial melting documented in this volume might be overcome by the application of alternative welding techniques, such as friction welding. Problems due to microsegregation may also be overcome by limiting the trace-impurity content of wrought and

cast materials and controlling the grain size, primarily in cast materials.

CDA 102, though prone to the effects of hydrogen sickness or porosity formation because of the reduction of entrapped cuprous oxide particles, could be employed as a container material if a suitable filler material with sufficient deoxidizing capabilities were used. The utilization of an alternate high-purity copper alloy, such as CDA 122, might preclude this requirement.

The aluminum bronze alloy, CDA 613, appears to have the most significant problems when welding is considered. The formation of an aluminum oxide scale and the inclusion of oxide particles with inadequate inert-gas shielding could significantly affect weld integrity. The almost complete loss of ductility in the temperature range of 400 to 600°C and the resulting possibility of hot cracking suggest that this alloy might not be suitable for high-level nuclear-waste container applications.

5. Acknowledgments

This work was performed under the auspices of the U.S. Department of Energy by Lawrence Livermore National Laboratory under contract No. W-7405-ENG-48, and was supported by the Yucca Mountain Project.

6. References

1. D. B. Bullen, G. E. Gdowski, *Survey of Degradation Modes of Candidate Materials for High-Level Radioactive-Waste Disposal Containers, Vol. 1, Phase Stability*, Lawrence Livermore National Laboratory, Livermore, California, UCID-21362 Vol. 1 (1988). NNI.881220.0035
2. G. E. Gdowski, D. B. Bullen, *Survey of Degradation Modes of Candidate Materials for High-Level Radioactive-Waste Disposal Containers, Vol. 2, Oxidation and Corrosion*, Lawrence Livermore National Laboratory, Livermore, California, UCID-21362 Vol. 2 (1988). NNI.881220.36
3. G. E. Gdowski, D. B. Bullen, *Survey of Degradation Modes of Candidate Materials for High-Level Radioactive-Waste Disposal Containers, Vol. 6, Effects of Hydrogen in Austenitic and Copper-Based Alloys*, Lawrence Livermore National Laboratory, Livermore, California, UCID-21362 Vol. 6 (1988). NNI.881220.0040
4. J. C. Farmer, R. A. Van Konynenburg, R. D. McCright, D. B. Bullen, *Survey of Degradation Modes of Candidate Materials for High-Level Radioactive Waste Disposal Containers, Vol. 3, Localized Corrosion and Stress Corrosion Cracking of Austenitic Alloys*, Lawrence Livermore National Laboratory, Livermore, California, UCID-21362 Vol. 3 (1988). NNI.881220.37
5. J. C. Farmer, R. A. Van Konynenburg, R. D. McCright, G. E. Gdowski, *Survey of Degradation Modes of Candidate Materials for High-Level Radioactive-Waste Disposal Containers, Vol. 4, Stress Corrosion Cracking of Copper-Based Alloys*, Lawrence Livermore National Laboratory, Livermore, California, UCID-21362 Vol. 4 (1988). NNI.881220.38
6. J. C. Farmer, R. D. McCright, R. A. Van Konynenburg, *Survey of Degradation Modes of Candidate Materials for High-Level Radioactive Waste Disposal Containers, Vol. 5, Localized Corrosion of Copper-Based Alloys*, Lawrence Livermore National Laboratory, Livermore, California, UCID-21362 Vol. 5 (1988). NNI.881220.39
7. 1983 Annual Book of ASTM Standards, Section 2, Nonferrous Metal Products, Volume 02.01, Copper and Copper Alloys, ASTM, Philadelphia, Pennsylvania, 1983, pp. 1246-1272. NNA.890915.0164
8. M. Hansen, K. Anderko, *Constitution of Binary Alloys*, 2nd ed., McGraw-Hill Book Company, New York, 1958, pp. 84-90. NNA.891009.0004
9. J. Kwarciaik, Z. Bojarski, H. Morawiec, "Phase Transformation in Martensite of Cu-12.4%Al," *Journal of Materials Science*, Vol. 21, No. 3, March 1986, pp. 788-792. NNA.890921.007
10. *Metals Handbook*, 8th ed., American Society for Metals, Metals Park, Ohio (1973), Vol. 8, p. 294.
11. E. A. Feest, R. H. Doherty, "The Cu-Ni Equilibrium Phase Diagram," *Journal of the Institute of Metals*, Vol. 99 (1971), pp. 102-104.
12. C. H. Thornton, S. Harper, J. E. Bowers, *A Critical Survey of Available High Temperature Mechanical Property Data for Copper and Copper Alloys*, International Copper Research Association, New York (December 1983), Chaps. 2.1, 2.13, 2.21. NNA.890921.0080
13. D. C. Moore, E. A. Taylor, "Welding of Copper and Copper Alloys by the Inert-Gas-Shielded Self-Adjusting Metal-Arc Process," *British Welding Journal*, Vol. 2, October 1955, pp. 427-442. NNA.890915.0165
14. C. A. Terry, E. A. Taylor, "Welding of Cupro-Nickel and Aluminium-Bronze Alloys," *British Welding Journal*, Vol. 5, May 1958, pp. 211-225. NNA.890915.0166
15. V. P. Weaver, J. Imperati, *Copper and Copper Alloys for Pressure Vessels*, Welding Research Council, New York, Welding Research Council Bulletin No. 73 (November 1961). NNA.890915.0167
16. K. Wold, "Welding of Coppers and Copper Alloys," *Metal Progress*, Vol. 108, No. 8, December 1975, pp. 43-47. NNA.890915.0168
17. R. J. C. Dawson, *Welding of Copper and Copper Base Alloys*, Welding Research Council, New York, Welding Research Council Bulletin No. 287 (September 1983). NNA.890915.0169
18. J. F. Lancaster, *Metallurgy of Welding*, George Allen & Unwin, London, 1980, pp. 207-211. NNA.890915.0170
19. E. G. West, *Copper and Its Alloys*, John Wiley & Sons, New York, 1982, pp. 189-194. NNA.890831.0060

20. C. E. Witherell, Lawrence Livermore National Laboratory, Livermore, California, private communication (June 17, 1988). NNA.890928.0052
21. E. Mattsson, F. Schuckher, "An Investigation of Hydrogen Embrittlement of Hydrogen in Copper," *Journal of the Institute of Metals*, Vol. 87, 1958-59, pp. 241-247. NNA.890921.0086
22. E. Kauczor, "Hydrogen Embrittlement of Copper," *Metall*, Vol. 19, No. 11, November 1965, pp. 1185-1187. NNA.890921.0086
23. C. E. Ransley, "The Diffusion of Oxygen in Copper," *Journal of the Institute of Metals*, Vol. 65, 1939, pp. 147-172.
24. J. Peterseim, G. Thummes, H. H. Mende, "Reduction of the Residual Resistivity of Thin Copper-Wires by Internal Oxidation," *Zeitschrift für Metallkunde*, Vol. 70, No. 4, April 1979, pp. 266-270. NNA.890921.0089
25. E. Albert, R. Kirchheim, E. From, *Gase in Metallen*, Deutsche Gesellschaft für Metallkunde, Darmstadt, F.R.G. (1979), pp. 45-49. NNA.890921.0090
26. B. Hammer, D. Lenz, P. Reimers, T. Dudzus, B. F. Schmitt, "Die Löslichkeit des Sauerstoffs in Reinstkupfer," *Metall*, Vol. 38, No. 1, January 1984, pp. 41-45. NNA.890921.0091
27. E. C. Mantle, "Welding with Aluminum Bronzes," *Engineering*, Vol. 172, October 1951, p. 443. NNA.890915.0171
28. J. F. Lancaster, D. Slater, "The Cracking of Aluminium Bronze Welds," *British Welding Journal*, Vol. 5, May 1958, pp. 238-244. NNA.890915.0172
29. K. J. Clews, "Metallurgical Aspects of Aluminium Bronze Welding Problems," *British Welding Journal*, Vol. 12, No. 3, March 1965, pp. 126-144. NNA.890915.0173
30. K. J. Clews, "Cracking of Aluminium Bronze Plate During Welding," *British Welding Journal*, Vol. 12, No. 6, June 1965, pp. 301-309. NNA.890915.0174
31. K. J. Clews, "Elevated Temperature Properties of Aluminium Bronze (Alloy D) Parent Metal, Rod and Weld Metal," *British Welding Journal*, Vol. 13, No. 8, August 1966, pp. 476-483. NNA.890916.0175
32. N. C. Ashton, "Fabricating and Welding Aluminum Bronze," *Metal Construction*, Vol. 11, No. 8, August 1979, pp. 392-394. NNA.890915.0176
33. D. Medley, Wisconsin Centrifugal Inc., letter to C. E. Witherell, Lawrence Livermore National Laboratory, Livermore, California (May 10, 1988).
34. L. H. Hawthorne, R. F. Burth, "Welding the Cupro-Nickels by the Inert-Gas-Shielded Arc Processes," *Welding Journal*, Vol. 35, August 1956, pp. 401s-408s. NNA.890915.0177
35. C. E. Witherell, "Some Factors Affecting the Weldability of the Cupro-Nickels," *Welding Journal*, Vol. 39, No. 9, September 1960, pp. 411s-416s. NNA.890915.0178
36. G. E. Grotke, "Cast-Pin-Tear and Hot-Ductility Tests of High Nickel and Cu-Ni Alloys," in *Proceedings of the Symposium on Effects of Minor Elements on the Weldability of High-Nickel Alloys*, Welding Research Council, 1967, p. 138. NNA.890915.0179
37. S. J. Matthews, "Weldability Observations in 70/30 Copper-Nickel Tubeshell Material," *Welding Journal*, Vol. 47, No. 4, April 1968, pp. 155s-161s. NNA.890915.0180
38. J. W. Lee, E. E. Nichols, S. Goodman, "Varestraint Testing of Cast 70Cu-30Ni Alloy," *Welding Journal*, Vol. 47, No. 8, August 1968, pp. 371s-377s. NNA.890915.0181
39. W. F. Savage, E. F. Nippes, T. W. Miller, "Microsegregation in 70Cu-30Ni Weld Metal," *Welding Journal*, Vol. 55, No. 6, June 1967, pp. 165s-173s. NNA.890915.0182
40. W. F. Savage, E. F. Nippes, T. W. Miller, "Microsegregation in Partially Melted Regions of 70Cu-30Ni Weldments," *Welding Journal*, Vol. 55, No. 7, July 1976, pp. 181s-187s. NNA.890915.0183
41. W. F. Savage, E. F. Nippes, J. E. Casteras, "Effect of Alloying Additions on the Weldability of 70Cu-30Ni," *Welding Journal*, Vol. 57, No. 12, December 1978, pp. 375s-382s. NNA.890915.0184
42. G. Bertelli, M. Scasso, "Welding of Copper-Nickel Alloys," *Rivista Italiana della Saldatura*, Vol. 37, No. 2, March/April 1985, pp. 77-82. NNA.890915.0185
43. C. E. Witherell, Lawrence Livermore National Laboratory, Livermore, California, private communication (June 17, 1988). NNA.890928.0052
44. K. J. A. Kundig, *Fabrication Alternatives for Manufacturing Copper and Copper Alloy Nuclear Waste Containers*, report to Lawrence Livermore National Laboratory from the Copper Development Association, Inc. (May 30, 1986). NNA.890915.0186

45. K. O. Stein, *Closure Development for High-Level Nuclear Waste Containers for the Tuff Repository, Phase 1 Final Report*, Babcock & Wilcox Report BAW-2009 (October 1987).
46. K. O. Stein, *Fabrication Development for High-Level Nuclear Waste Containers for the Tuff Repository, Phase 1 Final Report*, Babcock & Wilcox Report BAW-2010 (October 1987).
47. R. J. C. Dawson, "Copper and Its Alloys: Welding—An Industrial Status Report," *Metal Construction*, Vol. 9, No. 1, January 1977, pp. 20–23. NNA.890915.0187
48. E. D. Nichols, "Copper and Its Alloys: Friction Welding," *Metal Construction*, Vol. 9, No. 1, January 1977, pp. 23–25. NNA.890915.0188
49. K. K. Wang, *Friction Welding*, Welding Research Council Bulletin No. 204, Welding Research Council, New York (April 1975). NNA.890915.0189

The following number is for Office of Civilian Radioactive Waste Management Records Management purposes only and should not be used when ordering this document:

Accession Number: NNA.891222.0313